Detection of intermediates in the TiO$_2$-assisted photodegradation of Rhodamine B under visible light irradiation

LI Jing-yi[1,2,*], MA Wan-hong[2], LEI Peng-xiang[2], ZHAO Jin-cai[2]

1. College of Chemistry and Chemical Engineering, Inner Mongolia University, Hohhot, Inner Mongolia 010021, China.
E-mail: lijingyicn@yahoo.com
2. Centre for Molecular Science, Institute of Chemistry, Chinese Academy of Sciences, Beijing 100080, China

Abstract

The photocatalytic degradation of dye Rhodamine B (RhB) in the presence of TiO$_2$ nanostripe or P25 under visible light irradiation was investigated. The degradation intermediates were identified using Infrared spectra (IR spectra), ^{1}H nuclear magnetic resonance (^{1}HNMR) spectra, and gas chromatography-mass spectroscopy (GC-MS). The IR and the ^{1}HNMR results showed that the large conjugated chromophore structure of RhB was efficiently destroyed under visible light irradiation in both the photocatalytic systems (TiO$_2$ nanostripe or P25 and Rhodamine B systems). GC-MS results showed that the main identified intermediates were ethanediotic acid, 1,2-benzenedicarboxylic acid, 4-hydroxy benzoic acid and benzoic acid, which were almost the same in the TiO$_2$ nanostripes and P25 systems. This work provides a good insight into the reaction pathway(s) for the TiO$_2$-assisted photocatalytic degradation of dye pollutants under visible light irradiation.

Key words: TiO$_2$; visible light irradiation; Rhodamine B (RhB)

Introduction

It is difficult to degrade the toxic pollutants which are harmful to environment and mankind. In the past, the photodegradation of organic pollutants under UV light irradiation has become a potential method for the removal of these pollutants and has been investigated extensively. However, the most critical obstacle toward its effective utilization is the relatively inefficient use of solar energy, for less than 5% (UV light) of the sunlight is absorbed by this photocatalyst while artificial UV light source is expensive. Therefore, many researchers attach great importance to the degradation of environmental pollutants using visible light or sunlight. In recent years, we have reported the photodegradation of dye pollutants in the presence of TiO$_2$ under visible light irradiation (Chen *et al.*, 2002; Li *et al.*, 2002a, b, 2007; Zhao *et al.*, 2002; Zhu *et al.*, 2005). According to their research, it is dye pollutants rather than TiO$_2$ that are excited by visible light. The excited dye pollutants transfer electrons to the conduction band of TiO$_2$. The oxygen molecules adsorbed on TiO$_2$ surface trap the conduction electron, yielding superoxide

radicals, which are subsequently converted into hydroxyl radicals and other oxygen radicals by protonation, disproportionation and reduction. These radicals are active oxidation agents which can degrade dye molecules. Nevertheless, rather than a straightforward oxidation reaction ending with complete oxidized products, like CO$_2$, H$_2$O and inorganic salts, the dye degradation is a complicated process which involves various possible routes depending on experimental parameters. For instance, we have recently investigated the photodegradation of Rhodamine B (RhB) with P25, TiO$_2$ nanorod and TiO$_2$ nanostripe under visible light irradiation (Zhu *et al.*, 2005; Li *et al.*, 2007) and found that the morphology and crystal structure of the TiO$_2$ catalysts have an important effect on the degradation activity of the catalysts. The comprehensive understanding of the degradation mechanism on the catalysts is essential for designing new and efficient photocatalysts that can work under visible light irradiation. In addition, so far as its application is concerned, another important question is the toxicity of degradation intermediates, which may cause more serious secondary pollution.

In the present study, to make clear the photocatalytic degradation of dye pollutants under visible light irradiation and to examine the toxicity of its intermediates, we investigated the intermediates formed during the TiO$_2$-assisted (P25 and TiO$_2$ nanostripe) photodegradation of Rhodamine B (RhB) under visible light irradiation by infrared spectra (IR spectra), ^{1}H nuclear magnetic resonance
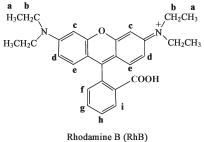
(¹HNMR) spectra and GC-MS spectra.

1 Experimental section

1.1 Materials

A commercial product of titania powder, P25, was kindly supplied by Degussa Co., which contains about 80% anatase and 20% rutile with BET specific surface area of about 50 m^2/g. TiO₂ nanostripe was prepared following the procedures described in reference (Li *et al.*, 2007). Deionized and doubly distilled water was used throughout this study. For reference, the structure of RhB is shown below.

Rhodamine B (RhB)

1.2 Photoreactor and light source

A 500-W halogen lamp (Institute of Electric Light Source, Beijing), as a visible light source, was positioned inside a cylindrical Pyrex glass vessel surrounded by a recirculating water jacket of Pyrex glass to cool the lamp. A cut-off filter was placed outside the Pyrex jacket to completely remove the light with wavelengths shorter than 450 nm and to ensure that the irradiation entering the reaction system was visible light only.

1.3 Procedures of sample analyses

Gas chromatography-mass spectroscopy (GC-MS, Trio-2000, Micromass, U.K.) with column BPX 70: size 28 m × 0.25 mm, quartz chromatographic column was used to determine the reaction intermidiate. Working cooditions; are as follows: sampling inlet temperature: 260°C; programming temperatures: 60–260°C at rate of 6°C/min; ion source temperature: 180°C; electron energy: 70 eV. Experiments were prepared as follows: several dispersions (25 ml of 2×10^{-5} mol/L; pH 2.5) consisting of RhB and 25 mg TiO₂ particulates were irradiated for different time intervals. When RhB lost its color, we added RhB again to reach the concentration of 2×10^{-5} mol/L. This operation was repeated until the total amount of RhB added is 1×10^{-4} mol/L. Subsequently, TiO₂ particles were removed by centrifuging at 4000 r/min. After removal of the solvent from the filtrates (below 323 K) by distilling under reduced pressures, the residues were dissolved in methanol. The obtained residues (before being dissolved in methanol, the residue was used directly) were also used to prepare specimens for infrared spectra (IR Bruker tensor 27, Germany; resolution rate: 4 nm; sample scanning time: 16 s; detector setting: RT-DlaTGS (Internal), KBr pelleting). Samples for ¹HNMR spectra (Bruker DMX-300, Germany; probe head: BBI; sampling point: 12048; scanning number: 8; spectra width: 8992.806 Hz; delaying time: 3 s; spectrometer frequency: 300 MHz) were also prepared using the dried residues, finally they were dissolved in D₂O.

2 Results and discussion

2.1 Infrared spectra

The IR spectra in Figs.1a and 1b show the photodegradation process of RhB in the presence of P25 and TiO₂
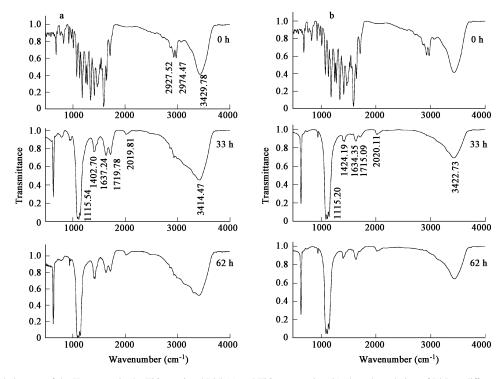

Fig. 1 Temporal changes of the IR spectra in the TiO₂-assisted P25 (a) and TiO₂ nanostripe (b) photodegradation of RhB at different irradiation times.

nanostripe illuminated by visible light irradiation. According to the literature (Liu and Zhao, 2000; Liu *et al.*, 2000; Wu *et al.*, 1998), the assignments for the RhB (before irradiation) are as follows: the bands at 3430 cm^{-1} are due to –OH stretch vibration, the bands at 2974, 2928 cm^{-1} are caused by –CH$_2$– and C–CH$_3$ stretch vibration, respectively. The peaks at 1590, 1528, 1468 cm^{-1} correspond to aromatic ring vibrations, while the 1341 cm^{-1} peak attributes to C-aryl bond vibration; the peak at 1720 cm^{-1} are due to C=O groups. The peak at 1646 cm^{-1} is caused by vibrations of the C–N bond and the heterocycle vibrations cause the peak ranging at 1530–1558 cm^{-1}. During the photodegradation, heterocycle vibrations disappear with irradiation. The peaks at 1720 and 1715 cm^{-1} remain, which are ascribed to C=O groups. The new strong peak at 1088–1145 cm^{-1} may be caused by –C–O–H stretch vibration. The IR results show that the large conjugated chromophore structure of RhB is destroyed under visible light irradiation, yielding smaller organic molecules.

2.2 Proton NMR spectra

^{1}HNMR spectra results of the final photodegradation products for the RhB, TiO$_2$ systems (P25 and TiO$_2$ nanostripes) are shown in Figs.2a and 2b. Spectrum 0 h (Fig.2a) shows the typical proton NMR signals of pure RhB (Liu and Zhao, 2000; Liu *et al.*, 2000; Wu *et al.*, 1998). The various protons in the structure of RhB are shown in the structure of RhB . The NMR signals of

the aromatic hydrogen atoms H$_c$, H$_d$, H$_e$, H$_f$, H$_g$, H$_h$ and H$_i$ (c, d, e, f, g, h, and i are the element H position in RhB structure) are located at δ6.53, 6.70–6.73, 6.99–7.02, 7.28–7.30, 7.60–7.65, 7.90–7.93 ppm, respectively. The NMR signals of H$_a$ and H$_b$ of the N-diethyl group appear at δ1.05–1.10, 3.39–3.42 ppm, respectively. During the photodegradation (Fig.2a), a series of new signals appear at δ1.25–1.28 (hydrogen atoms from the CH$_3$ and analogous groups) and δ2.52–3.19 ppm, whereas the characteristic signals of the N-diethyl group and the aromatic hydrogen atoms in RhB at δ1.05–1.10 (CH$_3$), 3.39–3.42 (CH$_2$) and δ6.53–7.93 ppm (aromatic protons) decreased remarkably. The ^{1}HNMR spectra for RhB/TiO$_2$ nanostripe system are shown in Fig.2b. In the course of photodegradation (Fig.2b), a series of new signals appear at δ2.85–3.98 ppm, 8.31 ppm, 9.31 ppm (carboxylic acids –OH). The above NMR results further indicate that the breakup of chromophoric structure of RhB occurs during the initial irradiation stage.

2.3 GC-MS measurements

The GC-MS was also used to detect the intermediates of RhB, P25 and RhB, TiO$_2$ nanostripe illuminated by visible light irradiation and to provide an additional evidence for the photoreaction pathways. The GC-MS results of the final photodegradation products of RhB after visible light irradiation of 41 h in P25 and TiO$_2$ nanostripes systems are shown in Figs.3 and 4, respectively, and
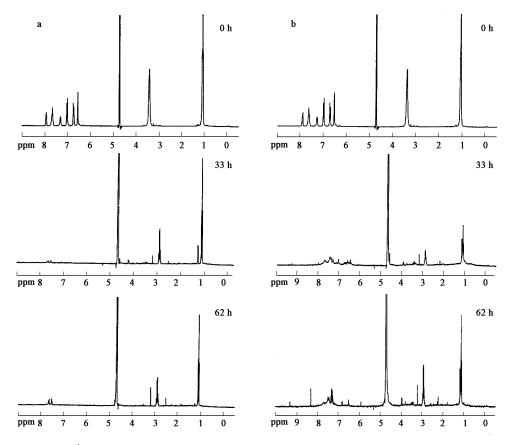

Fig. 2 Temporal variation of the ^{1}HNMR spectra in the course of TiO$_2$-assisted P25 (a) and TiO$_2$ nanostripe (b) photodegradation of a D$_2$O solution of RhB at different irradiation times (the strong signal at about 4.7 ppm is that of D$_2$O present in deuterated D$_2$O).
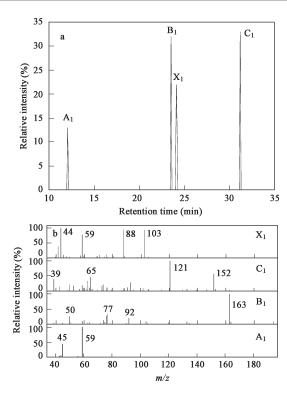
Fig. 3 GC chromatogram analysis from the TiO₂-assisted (P25) photodegradation of RhB after visible light irradiation of 41 h (a) and mass spectra of the species in the GC in Fig.3a (b).

summarized in Table 1. Four peaks were observed in the GC for P25-mediated system (Fig.3a). The predominant peaks A_1, B_1 and C_1 (Fig.3a) are analyzed in detail by mass spectroscopy (Fig.3b). The product was identified by comparing the molecular ion and mass fragmentation pattern with those reported in the GC-MS library. The major products corresponding to peaks A_1, B_1 and C_1 are ethanediotic acid (A_1), 1,2-benzenedicarboxylic acid (B_1) and 4-hydroxy benzoic acid (C_1), respectively.
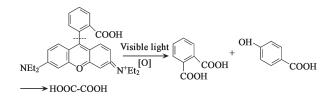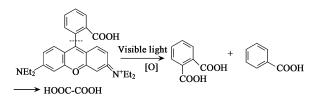
The reaction pathway is as follows:

Fig.4 illustrates the GC-MS results of the final products of RhB photodegradation in the TiO₂ nanostripe system. There were seven peaks observed (Fig.4a). The peaks A_2 and C_2 for TiO₂ nanostripe have the same retention time

Table 1 GC-MS results of the P25 and TiO₂ nanostripes after visible light irradiation of 41 h

Sample Components	P25			TiO₂ nanostripe		
	A_1	B_1	C_1	A_2	B_2	C_2
Retention time (min)	12.07	23.52	31.17	12.05	15.50	23.49
Relative peak area (%)	13	32	33	16	4	54

in the GC as peaks A_1 and B_1 in the P25 case, respectively. The analysis by mass spectroscopy confirms that the components A_2 and C_2 in Fig.4a have identical mass spectroscopy patterns with that of the A_1 and B_1 (Fig.3b), that is, the identified products are also ethanediotic acid (A_2) and 1,2-benzenedicarboxylic acid (C_2). The peak which appeared at a retention of 15.5 min (B_2) is assigned to benzoic acid, which was not found in the P25 system. Instead, a hydroxylated product (4-hydroxy benzoic acid (C_1)) was observed in P25 case. It is indicated that the main identified products in both systems are nearly the same. The reaction pathway is as follows:

It should also be mentioned that, in both the photocatalytic systems, several GC-MS peaks (X_1 for TiO₂ system, X_1–X_4 for TiO₂ nanostripes system) can not be identified. Although the identified products are almost the same in both photocatalyst systems, GC-MS peaks for the unidentified products are completely different in both the retention time and the mass spectroscopy patterns, which suggest the existence of different products and the difference of photocatalytic pathways between the P25 and TiO₂ nanostripe photocatalyst. The phenomena may be caused by the different morphology and crystal structure of P25 and TiO₂ nanostripe (Li *et al*., 2007). The BET specific surface area of the calcined nanostripes is 469 m²/g, which
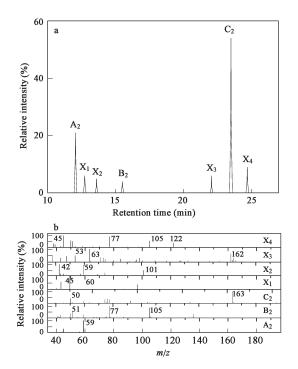

Fig. 4 GC chromatogram from the TiO₂-assisted (TiO₂ nanostripe) photodegradation of RhB after visible light irradiation of 41 h (a) and mass spectra of the species observed in the GC shown in Fig.4a (b).

is much bigger than that of P25. The nanostripes are about 10 nm wide and over 100 nm long by TEM results. They are different from P25, which are particles with a diameter of about 30–50 nm. From Raman and XRD results (data not shows), we know that TiO_2 nanostripes are neither anatase nor rutile but a sort of titanate. The results may well explain why their reaction pathways are different under the different reaction conditions.

During the photodegradation under visible light irradiation, RhB dye is adsorbed on the TiO_2 surface through a carboxylic group (because pH value of the dispersion system is acidic). The products of B_1, C_1, B_2 and C_2 from RhB irradiation (shown in Figs.3 and 4) indicate that the destruction of chromophore structure predominates, and de-ethylation is minor in the photodegradation of RhB under visible light irradiation. The toxicity of the detected main degradation products (small molecule carboxylates besides CO_2 and H_2O) is rather low, which also implies that the technique of TiO_2-assisted photodegradation of dye pollutants under visible light irradiation could be used to transform the toxic dye pollutants to low-toxic or non-toxic compounds. But under ultraviolet light irradiation (Liu and Zhao, 2000; Liu *et al.*, 2000), they should have the same intermediates as that under visible light irradiation, for the former, the intermediates can further be degraded into smaller molecules. However, for the latter, the degraded fragments underwent no further decomposition with further irradiation by visible light after the dispersions were completely decolored.

3 Conclusions

In this study, the photodegradation intermediates of dye Rhodamine B under visible light irradiation in the presence of two photocatalysts (P25 and TiO_2 nanostripe) are examined. It is indicated that, in both the photocatalytic system, the large conjugated chromophore structure of dye pollutants can be effectively destroyed under visible light irradiation. The detected degradation intermediates are predominantly the small molecule organic acids (such as ethanediotic acid, 1,2-benzenedicarboxylic acid, 4-hydroxy benzoic acid and benzoic acid), which are observed in both the two photocatalytic systems. However, from the GC-MS, there exists much difference in the

intermediates for the two systems. Although the specific structure is not identified at the present stage, it is certain that the difference can be caused by the different morphology and crystal structure of P25 and TiO_2 nanostripe. This study not only provides an insight into the reaction pathway(s) of the photodegradation of dye pollutants, and what's more, it also indicates that the degraded intermediates, besides CO_2, H_2O and inorganic salts, are mainly low- or non-toxic colorless organic acids, which are desirable for its practical application in treatment of dye pollutants.

References

Chen C C, Li X Z, Ma W H *et al.*, 2002. Effect of transition metal ions on the TiO_2-assisted photodegradation of dyes under visible irradiation: A probe for the interfacial electron transfer process and reaction mechanism[J]. J Phys Chem B, 106(2): 318–324.

Li J Y, Chen C C, Zhao J C *et al.*, 2002. Photodearadation of dye pollutants on TiO_2 nanoparticles dispersed in silicate under UV-Vis irradiation[J]. Appl Catal B, 37: 331–338.

Li J Y, Chen C C, Zhao J C *et al.*, 2002. Photodegradation of dye pollutants on TiO_2 pillared bentonites under UV light irradiation[J]. Sci in China B, 45(4): 445–448.

Li J Y, Ma W H, Chen C C *et al.*, 2007. Photodegradation of dye pollutants on one-dimensional TiO_2 nanoparticles under UV and visible irradiation[J], J Mole Catal A: Chem, 261: 131–138.

Liu G M, Zhao J C, 2000. Photocatalytic degradation of dye Sulforhodamine B: A comparative study of photocatalysis with photosensitization[J]. New J Chem, 24: 411–417.

Liu G M, Li X Z, Zhao J C *et al.*, 2000. Photooxidation pathway of Sulforhodamine-B. Dependence on the adsorption mode on TiO_2 exposed to visible light radiation[J]. Environ Sci Technol, 34(18): 3982–3990.

Wu T X, Liu G M, Zhao J C *et al.*, 1998. Photoassisted degradation of dye pollutants V: Self photosensitized oxidative transformation of RhB under visible light irradiation in aqueous TiO_2 dispersions[J]. J Phys Chem, 102(30): 5845–5851.

Zhao W, Chen C C, Li X Z *et al.*, 2002. Photodegradation of Sulorhodamine-B dye in platinum as a functional co-catalyst[J]. J Phys Chem B, 106(19): 5022–5028.

Zhu H Y, Li J Y, Zhao J C *et al.*, 2005. Photocatalysts prepared from layered clays and titanium hydrate for degradation of organic pollutants in water[J]. Appl Clay Sci, 28: 79–88.